

Retrofitting a brick wall using vacuum insulation panels: measured hygrothermal effect on the existing structure

Pär Johansson, Lic.Tech. ¹
Stig Geving, Professor ²
Carl-Eric Hagentoft, Professor ¹
Bjørn Petter Jelle, Professor ^{2,3}
Egil Rognvik ³
Angela Sasic Kalagasidis, Assistant Professor ¹
Berit Time, Ph.D. ³

¹ Chalmers University of Technology, Sweden

² Norwegian University of Science and Technology (NTNU), Norway

³ SINTEF Building and Infrastructure, Norway

KEYWORDS: *listed building, brick wall, interior insulation, vacuum insulation panel, measurement, laboratory, driving rain*

SUMMARY:

Old listed buildings need to be retrofitted to reduce the energy use for heating. Vacuum insulation panels (VIPs) require less thickness than conventional insulation materials to reach the same thermal resistance. The aim of this paper is to investigate the hygrothermal performance of a brick wall with wooden beam ends after it was insulated on the interior with VIPs. The paper presents the first part of a laboratory study where a brick wall was built in the laboratory and exposed to simulated driving rain. Different measurement techniques of the relative humidity in the construction have been used. The relative humidity in the wall increased substantially when exposed to driving rain. The moisture content in the wooden beams also increased. However, it has not been possible to fully determine the influence by the added insulation layer. It is clear that the drying capacity to the interior side is substantially reduced. These investigations are ongoing and will be reported in future publications.

1. Introduction

In Europe, the majority of the future building stock has already been built. The increasing energy prices and the pressure to reduce the energy use in society urge for energy retrofitting measures in the existing building stock (IEA 2013). External walls of old buildings in Sweden and Norway often have a low thermal resistance in comparison to current standards. In Swedish buildings built before 1960, the average U-value of the walls is 0.58 W/(m²·K) (Boverket 2009) while it is 0.9 W/(m²·K) for at least 100 000 Norwegian buildings from before 1945 (Thyholt *et al.* 2009). For retrofitted walls the general target U-value is 0.18 W/(m²·K) in Sweden (Boverket 2011) and 0.22 W/(m²·K) in Norway (KRD 2010). Many old buildings are considered to be of great historical value and are protected for their external appearance which limits the possible retrofitting measures. Retrofitting on the exterior side of the wall is, in many cases, not allowed so the only possible solution is to add interior insulation. The available additional thickness of the wall is limited by the allowed reduction in rentable internal floor area. Novel highly efficient thermal insulation materials such as vacuum insulation panels (VIPs) increases the thermal resistance of the wall compared to conventional insulation materials with the same thickness. The thermal resistance of a VIP is 5-10 times higher than for conventional insulation materials (Baetens *et al.* 2010), reducing the required thickness to reach a targeted thermal resistance.

VIPs are rigid panels which, unlike most insulation materials, cannot be adapted on the construction site and have to be preordered in the correct dimensions. They are sensitive to damages which could lead to puncturing and a fivefold increase in thermal conductivity. Therefore special care has to be taken in all stages of the construction process to avoid damaged VIPs. Also, thorough hygrothermal investigations are needed to ensure that the relative humidity in the wall is below the critical levels for mold growth and dry rot fungi in wood and freeze thaw damages in brick and mortar.

When retrofitting old buildings, the prerequisites are given by the existing construction. The intermediate floors in old brick buildings are often carried by wooden beams which are embedded in the brick. Mold and dry rot can damage the wooden beams and the risk for that is higher when interior insulation is added because of the higher relative humidity in the wall. Driving rain raises the moisture content in the wall and wooden beam ends, increasing the risk for damages. Also air leakages from the interior into the area around the wooden beam ends can transport moist air from the interior which will raise the moisture content even higher (Kehl *et al.* 2013). Unprotected brick walls may also have freeze-thaw damages. The movement of water through brick masonry has many important consequences in building constructions and it has therefore been studied by a number of authors, e.g. Hall (1977) and Brocken (1998). While the majority of these studies involved water suction experiments from a free water surface, large scale experiments where water suction in brick walls is studied during a real or artificial rain load, such as presented by Abuku *et al.* (2009) and Piaia *et al.* (2013), are rare. To the knowledge of the authors, similar studies for brick masonry are not available.

The aim of this paper is to investigate the hygrothermal performance of a brick wall with wooden beam ends after the wall was insulated on the interior side with VIPs. The brick wall was built in laboratory according to the methods used in the late 19th century to the early 20th century in Sweden and Norway. Wooden beam ends were studied since these are a known risk area when insulating brick walls (Kehl *et al.* 2013; Rasmussen 2010; Ueno 2012). The wall was tested in a large-scale building envelope climate simulator where it was exposed to a temperature gradient and cycling climate with driving rain. In the first sequence, the wall without interior insulation was tested. Before the second sequence VIPs were added to the interior of the wall. A pre-study using the hygrothermal simulation tool WUFI 2D was presented by Johansson *et al.* (2013) where suitable materials, wall layout and testing climate were proposed. The study is part of a research project which is run in cooperation between Chalmers University of Technology in Gothenburg, Sweden, the Norwegian University of Science and Technology (NTNU) and SINTEF Building and Infrastructure, in Trondheim, Norway.

2. Wall layout and material selection

A common wall thickness in brick buildings from the late 19th century is 380 mm which is equal to 1.5 bricks thick walls. The brick walls of multiple floors often have wooden beams inserted around 200 mm into the brickwork to carry the intermediate floors (Kvande & Edvardsen 2013). In the pre-study, Johansson *et al.* (2013) studied three wall thicknesses, 120 mm, 250 mm and 380 mm, to investigate the possibility to decrease the (expensive) testing time by using a thinner wall in the laboratory study. It was found that the moisture accumulation rate was not decreasing linearly with increasing thickness, but had a more exponential relationship. However, the same water flow was found during wetting for the different wall thicknesses. Therefore, the same conclusions could be drawn by using a 250 mm thick brick wall as for using a 380 mm thickness. The schematics of the brick wall built in the laboratory and investigated in this paper are presented in FIG 1.

Two VIP sizes, 20 mm thick, were used in the study, larger 600x1 000 mm and smaller 500x600 mm, as shown in FIG 1. Three types of sensors were installed in the wall to monitor the wetting and drying; 10 relative humidity sensors (E+E Elektronik EE060), 8 Sahlén sensors (wood moisture sensors) and 12 resistance moisture meters (pin-type). The relative humidity sensors measure the relative humidity and temperature in the range of 0-100% and -40-60°C. They were located in the mortar between the bricks, see FIG 2b, together with the Sahlén sensors. These measure the mass percentage moisture in

birch wood inside the sensor which gives a measurement range of 60-100% relative humidity. The size of the relative humidity sensor is 116x12 mm (length, diameter) and the Sahlén sensor is 40x13 mm. The resistance moisture meters were made of two insulated metal pins located 25 mm apart, installed on three different locations in the wooden beams as shown in FIG 1. One sensor was drilled into the center of the beam at the interior surface of the wall (a). Two other sensors were installed 10 mm from the end of the beam, one with insulated pins in the center of the beam (b) and one on the wooden surface (c). The relative humidity sensors were monitored hourly in the first sequence and every 6 minutes in the second sequence by a computerized system. The Sahlén sensors and resistance moisture meters were monitored daily at the start of the climate sequence, and later every 2 days.

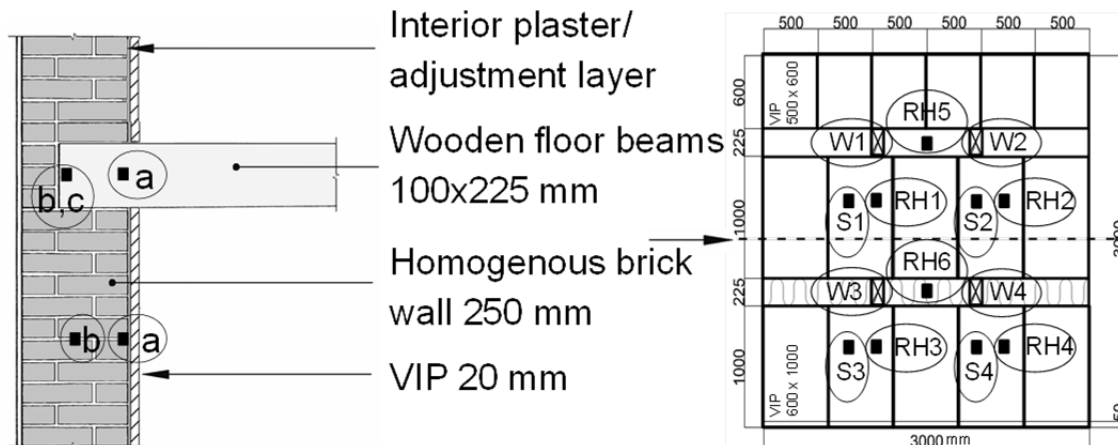


FIG 1. Left: schematics of the brick wall tested in the laboratory. The sensor locations at different depths of the wall are indicated by a, b and c. Right: measurements of the wall with the locations and sizes of the VIPs and sensor positions. RH = RH sensors, S = Sahlén sensors and W = resistance moisture meters. A layer of mineral wool was located around the two lower wooden beams. The horizontal dashed black line, indicated by an arrow, shows the symmetry line of the wall where a rubber strip was installed on the exterior side of the wall to break the water run-off.

The brick wall was built inside a 3x3 m steel frame to allow it to be moved from the laboratory to the climate simulator. The lower part of the frame was filled with 200 mm cellular glass insulation to insulate the lower boundary from the steel frame. The size of the bricks was 226x104x60 mm (length x width x height) and the thickness of the mortar joints between the bricks were 10-12 mm, see FIG 2a. The water accumulation in the upper part of the wall could interfere with the measurement results for the lower part of the wall. Therefore a rubber strip was installed on the exterior side of the wall to stop liquid water from being transported along the wall. Mortar was applied on the entire interior brick surface to make an even surface for attaching the VIPs. Four voids of each 100x225 mm, see FIG 2c, were created where the wooden beams were installed after the wall had dried. The gaps between the brick and wooden beams were sealed with a mix of modelling clay and beeswax. Around the two lower wooden beams, a layer of mineral wool was added to simulate the thermal resistance of the intermediate floor while the space around the two upper beams was left as it was, see FIG 1. A polyethylene foil was wrapped around the beams and over the space between them to simulate the vapor resistance of an intermediate floor, see FIG 2d. In the second sequence of the laboratory study, the interior side of the brick, between the intermediate floors, was covered by VIPs, see FIG 2e.

To resemble the properties of an old brick wall in the laboratory study it was essential to use a brick and mortar similar to what was used in Sweden and Norway in the late 19th century to the early 20th century. The modern brick types are formed by dry-pressing, molding or extruding the clay to form the wanted size and shape (Brick Industry Association 2006), giving other properties to the bricks than what manual production methods does. The liquid water transport coefficient is lower for modern bricks than for the historical bricks which are targeted in this study. The bricks and mortar used in the laboratory study were chosen based on the conclusions from the pre-study by Johansson *et al.* (2013).

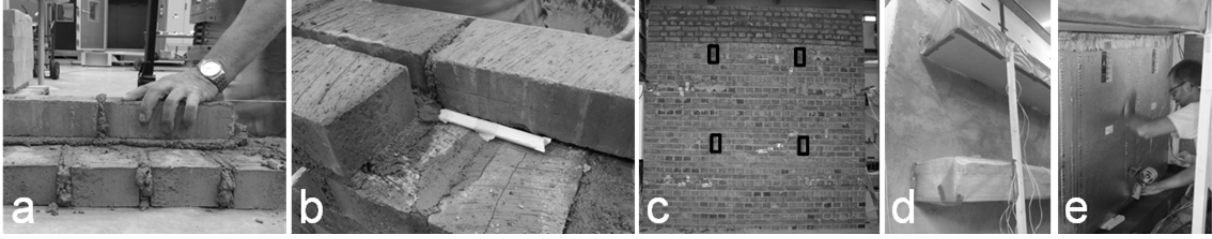


FIG 2. Photos from the construction of the wall in the laboratory. a: brick and mortar laid out, b: relative humidity sensor installed in the mortar in the middle of the wall, c: finished brick wall with the four voids for the wooden beams marked with black rectangles, d: wooden beams installed and wrapped in polyethylene foil, e: installation of the VIPs which were glued to the wall with taped edges.

The mortar type used to bind the bricks together has varied over time. Hydraulic lime mortar was used in the early days but later replaced by cement mortar and finally by mixtures of lime and cement mortar (Kvande & Edvardsen 2013). The liquid water transport coefficient is substantially larger for lime and cement mortars and hydraulic lime mortars than for pure cement mortar. Hydraulic lime mortar requires a longer curing time than a mixture of lime and cement mortar would. It was also expected to be more difficult to fully control the adhesion of the hydraulic lime mortar. Therefore, a lime and cement mortar was chosen which resembles the hygrothermal properties of the historic hydraulic lime mortar and minimizes the curing and adhesion times, allowing for faster construction.

3. Measurements of hygric properties of the brick and mortar

The hygric properties of the brick and mortar were tested in the laboratory of NTNU and SINTEF Building and Infrastructure in Trondheim, Norway. The procedures in the standards NS-EN ISO 15148 and NS-EN 1015-18 were followed using 6 samples each of the brick and mortar. The average values and standard deviations for the brick and mortar are presented in TABLE 1

TABLE 1. Measured hygric properties of the brick and mortar used in the laboratory study. The uncertainties are given as the standard deviation of the mean with a confidence interval of 68.3%.

Material	Density (kg/m ³)	A_w -value (kg/(m ² ·s ^{0.5}))	Moisture content at 75% RH (wt-%)	Moisture content at saturation (wt-%)
Brick	1 810 ± 30	0.19 ± 0.03	0.046 ± 0.004	13.1 ± 0.6
Mortar	1 670 ± 40	0.0655 ± 0.0004	2.04 ± 0.08	11.7 ± 0.2

The A_w -value is defined in NS-EN ISO 15148 as the short term liquid water absorption coefficient which is a measure of the rate of water absorption by e.g. driving rain on a material. To assess the liquid water transport coefficient, D_{ws} (m²/s) dependent on the moisture content, w (kg/m³), there is an approximate relationship between A_w and D_{ws} which is used in WUFI 2D (Fraunhofer IBP 2010):

$$D_{ws}(w) = 3.8 \cdot \left(\frac{A_w}{w_f} \right)^2 \cdot 1000 \left(\frac{w}{w_f} - 1 \right) \quad (1)$$

where A_w short term liquid water absorption coefficient (kg/(m²·s^{0.5}))
 w moisture content (kg/m³)
 w_f moisture content at saturation (kg/m³)

In order to use Equation (1), the moisture sorption isotherm for the material has to be defined. The approximate equation for the sorption isotherm based on measured data is (Fraunhofer IBP 2010):

$$w(\varphi) = w_f \cdot \frac{(b-1) \cdot \varphi}{b - \varphi} \quad (2)$$

where w_f moisture content at saturation (kg/m³)
 b fitting parameter (-)
 φ relative humidity (-)

The liquid water transport coefficient was calculated using Equation (1), based on the measurement results. The liquid water transport coefficients for the brick used in the laboratory study compared to the data from WUFI 2D (Fraunhofer IBP 2010) at 80% relative humidity (assuming $D_{ws} = 0$ m²/s at 0% RH with a linear relation to 80% RH) and at saturation are presented in TABLE 2.

TABLE 2. Liquid water transport coefficient at 80% relative humidity and at saturation for the brick used in this study compared to data from WUFI 2D (Fraunhofer IBP 2010).

Material	D_{ws} at 80% RH 10 ⁻⁹ (m ² /s)	D_{ws} at saturation 10 ⁻⁶ (m ² /s)
Measured brick	2.5	2.4
WUFI 2D	Masonry	1 600
	Extruded	7.5
	Historical	14
	Hand-formed	9.5
	Vienna 1900s	0.44

The liquid water transport coefficient increases with a factor of 1 000 when the moisture content in the brick used here becomes saturated. The relation is similar for the other brick types. “Historical” has the highest liquid water transport coefficient. The brick used in this study has a 100 times lower liquid water transport coefficient which is more in line with the properties of “Masonry” at saturation. The moisture diffusion resistance factor, μ (-), was not measured here but it is around 10-15 for most bricks (Fraunhofer IBP 2010).

The measured properties of the lime and cement mortar was similar to what is found in the WUFI 2D database for mortars of this type. The sorption isotherm was very similar to the sorption isotherm of the brick, but with a maximum moisture content of 195 kg/m³ compared to 237 kg/m³ in the brick. The liquid water transport coefficient was 1.5 · 10⁻⁹ at 80% relative humidity and 0.4 · 10⁻⁶ at saturation which is 60% and 18% of the brick. A parametric study of these different properties was performed by Johansson *et al.* (2013) which showed that the capillary active bricks gave a faster wetting of the wall.

4. Climate simulator and climate sequence

To make the results of the laboratory study applicable to the conditions in Gothenburg (Sweden) and Bergen (Norway), the climate sequence was based on the climate in these cities. They are both located close by the sea which means a large portion of driving rain will hit the façades of the buildings. Measurements of the amount of rain during a rain event were used as input. The climate simulator is designed to generate a controlled dynamic climate condition on both sides of the brick wall. On the interior side a constant temperature of 25°C and relative humidity of 40% was chosen.

The temperature and relative humidity was 5°C and 70% on the exterior side in the first sequence. In the second sequence it had to be changed to 10°C and 90% relative humidity because the equipment was overloaded and broke down during the first sequence. The rain period in the first sequence was supposed to be four hours long, but due to equipment malfunction the rain was not turned off in time but first after 14 hours. In the second sequence the rain period was reduced to 30 minutes since the rain intensity and the rate of the capillary suction were much higher than anticipated. The rain amount hitting the wall was 5 mm/hour, i.e. 5 l/(m²·h). After the wetting sequence, the drying climate was 10°C and 60% on the exterior side and kept at 25°C and 40% on the interior side. After 1 month drying with VIPs on the interior side of the wall, the panels were removed to allow for drying out from both sides of the wall. The climate was then changed to 40°C and 10% relative humidity on both sides.

5. Results of the hygrothermal measurements in the climate simulator

The plans for the measurements in the climate simulator had to be changed during the course of running the experiment. The malfunction during the first climate sequence meant that the wall was saturated after a very short time and also the interior side of the wall was wet. All the relative humidity sensors in the wall showed a relative humidity of 100% within less than 36 hours. The temperature could not be kept constant during this sequence so the temperature in the wall varied between 8.2°C and 21.2°C which makes an evaluation of the moisture measurement results complicated.

During the second sequence, the equipment worked more in line with the expectations. The temperature was kept constantly around 10°C on the exterior side of the wall which gave a temperature between 9.4°C and 11.2°C in the middle of the the wall. The measurements of the relative humidity in the wall during the second climate sequence are presented in FIG 3.

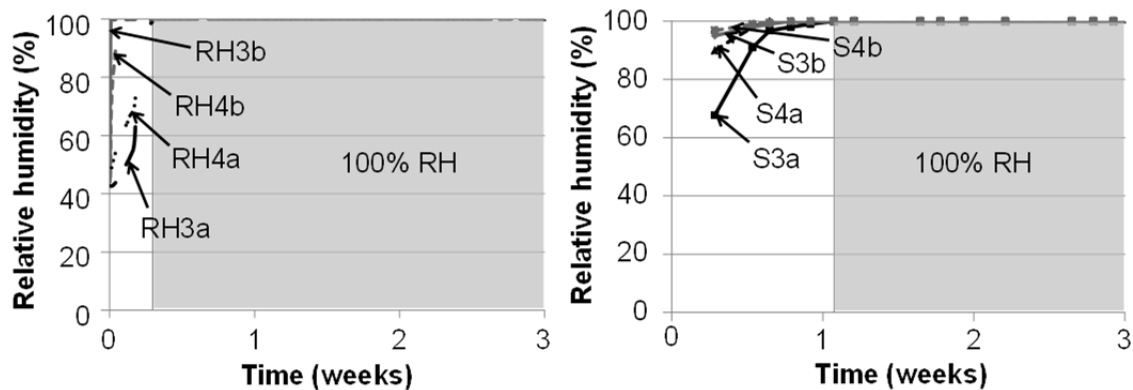


FIG 3. Relative humidity in the wall. Left: relative humidity measured with the relative humidity sensors. Right: relative humidity measured with the Sahlén sensors translated from the wood moisture content by using the sorption isotherm for birch wood. The sensors are located in the mortar in the middle of the wall (RH3b, RH4b, S3b, S4b) and in the mortar in the inner part of the brick wall (RH3a, RH4a, S3a, S4a). The Sahlén sensor only measures relative humidity above 60%.

It is clear that the moisture sensors in the middle of the wall are reached by the moisture faster than the sensors in the inner part of the brick wall. The Sahlén sensors show a significantly slower increase in relative humidity in the wall since the sensors uses a wooden material that has to absorb the moisture before the sensor can register the increasing moisture content. Also here, the relative humidity increases slower in the inner part of the brick wall in the first few days, but is then equal as in the middle of the wall. The relative humidity in the four wooden beams is shown in FIG 4.

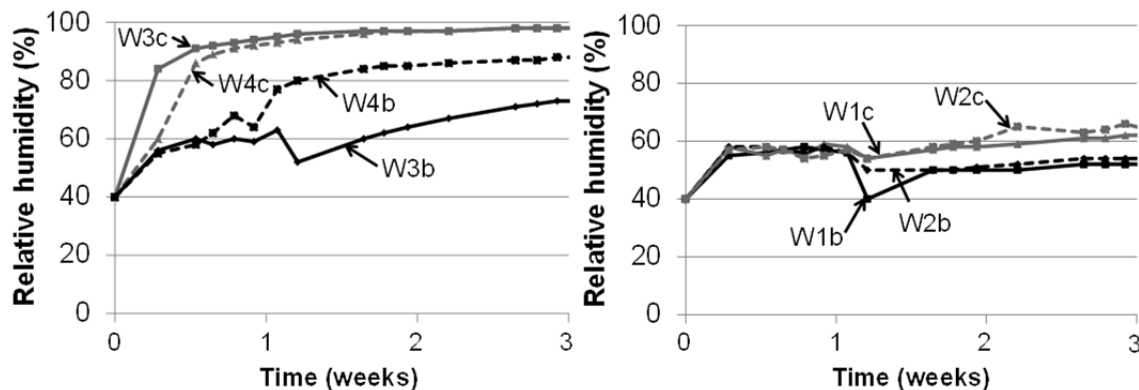


FIG 4. Relative humidity in the beams translated from the wood moisture content by using the sorption isotherm for spruce, in the middle of the beam end (b) and at the surface of the beam end (c). Left: lower beams (with mineral wool). Right: upper beams (without mineral wool).

There is a large difference between the relative humidity in the beams in the upper and lower part of the wall. This difference may partly be caused by the mineral wool insulation which is placed around the two lower beams, but not around the upper ones. The higher temperature in the wall results in a lower relative humidity, but this effect cannot explain the large difference on its own. The relative humidity sensors and Sahlén sensors in the upper part of the wall also showed a significantly lower relative humidity than what is shown for the lower part in FIG 3. The reason for this behavior is not clear. Part of it might be caused by the force of gravity on the liquid water flow.

6. Conclusions

A laboratory study with a brick wall built in the laboratory and exposed to simulated driving rain in a large-scale building envelope climate simulator was conducted. The relative humidity in the wall increased substantially when exposed to driving rain. As expected from the simulations in the pre-study, the moisture increased faster in the mortar in the middle of the wall compared to in the inner part. The brick and mortar was more capillary active than expected. The lower part of the wall had a higher relative humidity which could be caused by the force of gravity, acting on the liquid water flow. The different sensors gave consistent results, although the Sahlén sensor is more appropriate to be used in measurements where the relative humidity is expected to change slower than what was the case in this study. In the wooden beams, the moisture content increased more in the end of the beam than close to the interior brick surface. Due to equipment malfunction, data from important measurement periods are missing, making it difficult to draw conclusions from the first sequence of the laboratory investigations. In the next phase of this project, a wall without VIPs will again be tested and compared to the wall with VIPs. The simulations will be compared to hygrothermal simulations.

7. Acknowledgements

The work is supported by The Swedish Research Council Formas, the Lars Hierta Memorial Foundation, and finally the Research Council of Norway and several partners through The Research Centre on Zero Emission Buildings (www.ZEB.no). Porextherm Dämmstoffe GmbH is acknowledged for supplying the vacuum insulation panels and Wienerberger and St-Gobain Weber are acknowledged for supplying the brick and mortar.

References

- Abuku, M., Blocken, B., & Roels, S. 2009. Moisture response of building facades to wind-driven rain: field measurements compared with numerical simulations. *Journal of Wind Engineering and Industrial Aerodynamics*, 97(5-6), 197-207.
- Baetens, R., Jelle, B. P., Thue, J. V., Tenpierik, M. J., Grynning, S., Uvsløkk, S., & Gustavsen, A. 2010. Vacuum insulation panels for building applications: A review and beyond. *Energy and Buildings*, 42(2), 147-172.
- Boverket. 2009. Så mår våra hus - redovisning av regeringsuppdrag beträffande byggnaders tekniska utformning m.m. (The state of our buildings - report of governmental mission on the technical design of buildings etc.). [In Swedish]. Karlskrona, Sweden: Boverket.
- Boverket. 2011. Regelsamling för byggande, BBR 2012 (Regulations for construction, BBR 2012). [In Swedish]. Karlskrona, Sweden: Boverket.
- Brick Industry Association. 2006. Manufacturing of Brick. Reston, Virginia, USA: The Brick Industry Association.
- Brocken, H. J. P. 1998. Moisture Transport in Brick Masonry: The Grey Area Between Bricks (Dissertation). Eindhoven, The Netherlands: Eindhoven University of Technology, Faculty of Architecture, Building and Planning, and Faculty of Applied Physics.

- Fraunhofer IBP. (2010). WUFI 2D Transient Heat and Moisture Transport (Version 3.3.2) [Computer Program]. Holzkirchen, Germany: Fraunhofer IBP.
- Hall, C. 1977. Water movement in porous building materials - I. Unsaturated flow theory and its applications. *Building and Environment*, 12(2), 117-125.
- IEA. 2013. Policy Pathway: Modernising Building Energy Codes. Paris, France: OECD/IEA and New York, NY, USA: United Nations Development Programme (UNDP).
- Johansson, P., Time, B., Geving, S., Jelle, B. P., Sasic Kalagasidis, A., Hagentoft, C.-E., & Rognvik, E. 2013. Interior insulation retrofit of a brick wall using vacuum insulation panels: design of a laboratory study to determine the hygrothermal effect on existing structure and wooden beam ends. *Proceedings of the 12th International Conference on Thermal Performance of the Exterior Envelopes of Whole Buildings*, Clearwater Beach, Florida, USA, December 1-5, 2013.
- Kehl, D., Ruisinger, U., Plagge, R., & Grunewald, J. 2013. Wooden beam ends in masonry with interior insulation - A literature review and simulation on causes and assessment of decay. *Proceedings of the 2nd Central European Symposium on Building Physics*, Vienna, Austria, September 9-11, 2013.
- KRD. 2010. Byggteknisk forskrift (TEK 10). FOR-2010-03-26-489 Forskrift om tekniske krav til byggverk (Building Code. Regulations on technical requirements for construction). [In Norwegian]. Oslo, Norway: Kommunal- og regionaldepartementet, Bolig- og bygningsavd.
- Kvande, T., & Edvardsen, K. I. 2013. Eldre yttervegger av mur og betong. Metoder og materialer (Older exterior brick and concrete walls. Methods and materials). [In Norwegian]. Oslo, Norway: SINTEF Building and Infrastructure.
- Piaia, J. C. Z., Cheriaf, M., Rocha, J. C., & Mustelier, N. L. 2013. Measurements of water penetration and leakage in masonry wall: Experimental results and numerical simulation. *Building and Environment*, 61, 18-26.
- Rasmussen, T. V. 2010. Post-Insulation of Existing Buildings Constructed Between 1850 and 1920. *Proceedings of the 11th International Conference on Thermal Performance of the Exterior Envelopes of Whole Buildings*, Clearwater Beach, Florida, USA, December 5-9, 2010.
- NS-EN 1015-18:2002. Methods of test for mortar for masonry - Part 18: Determination of water absorption coefficient due to capillary action of hardened mortar. Brussels, Belgium: European Committee for Standardization (CEN).
- NS-EN ISO 15148:2002. Hygrothermal performance of building materials and products - Determination of water absorption coefficient by partial immersion. Geneva, Switzerland: International Organization for Standardization (ISO).
- Thyholt, M., Pettersen, T. D., Haavik, T., & Wachenfeldt, B. J. 2009. Energy Analysis of the Norwegian Dwelling Stock. Subtask A - Internal working document. IEA SHC Task 37 Advanced Housing Renovation by Solar and Conservation: International Energy Agency, Solar Heating and Cooling Programme.
- Ueno, K. 2012. Masonry Wall Interior Insulation Retrofit Embedded Beam Simulations. *Proceedings of the Building Enclosure Science & Technology Conference, BEST 3: High Performance Buildings - Combining Field Experience with Innovation*, Atlanta, GA, USA, April 2-4, 2012.